The 4-parameter Compressible Packing Model (CPM) for sustainable concrete

G Roquier

The 4-parameter Compressible Packing Model (CPM) for sustainable concrete.

G. Roquier[1]

[1] Laboratoire Navier, 77420 Champs-sur-Marne, France, gerard.roquier@laposte.net

ABSTRACT: To reduce the environmental impact due to the CO_2-emission, it is necessary to optimize the concrete mix-design by reducing the amount of cement. In this case, analytical packing models are necessary to predict the packing density of a pile of grains. A new version of the Compressible Packing Model (CPM) (de Larrard *et al.*), the 4-parameter CPM, is introduced to predict the solid fraction of maximally dense disordered packings of bidisperse particles. It is apt to account for the loosening effect on big particles by interstitial small ones, and for the wall effect within assemblies of small particles near a big one, with moderate size ratios. The new theory is based on a specific treatment of configurations of one secondary class particle surrounded by dominant class neighbours. It has four parameters : wall effect and loosening effect coefficients, critical cavity size ratio and compaction index. The model proves its efficiency when compared to 780 results on various tested materials. The correlation coefficients between predicted and measured packing densities are very high: 99% for frictionless glass beads, 98,7% for spherical particles numerically simulated, 97,8% for natural aggregates and 96,4% for crushed aggregates. To predict the viscosity of the same grains in a high concentrated suspension compound of spherical, inert and rigid particles suspended in a Newtonian fluid, we resort to the iterative approach advocated by Farris and to the Krieger-Dougherty power-law relation for the relative viscosity. The theory was developed to highlight a new relation between relative viscosity and the solid volume fraction, compatible with Einstein's relation.

1 INTRODUCTION.

A sustainable concrete mix-design implies both the substitution of cement by various cementitious materials, the optimization of the aggregate skeleton to minimize the interparticular volume of voids to be filled with the cement paste and the reduction of the concrete quantity needed for a civil engineering structure by increasing its mechanical performance. The latter can be easily linked to the packing density which itself depends on the concrete formulation. This one is divided in two stages. In the first one, concrete can be considered as a high concentrated suspension that we want to maximize the packing density for a given workability. This one can be linked, on a simplified basis, to the viscosity. The second stage concerns the search of the best sustainability while ensuring that the concrete continues to meet requirements: reducing the environmental cost of the material while playing with the proportioning of superplasticizer to obtain the desired workability. This ambitious goal leads to use models. This article deals with the particle packing and the concrete rheology by calling upon the last generation of the Compressible Packing Model (CPM): the 4-parameter CPM. To achieve its sustainable revolution, the concrete calls upon science to become a high-tech material.

2 THE REFERENCE FRAME: THE COMPRESSIBLE PACKING MODEL (CPM).

Introduced by the works of Stovall, de Larrard, Buil (1986) and Sedran, de Larrard, Angot (1994), the CPM, developed by de Larrard (2000), is a tool used to predict the packing density of multicomponent mixtures, while taking into account placing conditions.

2.1 Virtual packing density of a binary mixture.

The real packing density corresponds to that obtained for a randomly dense packing. It depends on process used to fill and to compact the material inside the mould. If we consider a perfect placing process where each particle is placed one by one in its ideal location, the compaction index tends to infinity and the packing density reaches the virtual packing density. For a binary mixture "without geometrical interaction", the latter is calculated by distinguishing two domains: "large grains dominant" and "small grains dominant". In the first case, the small component is fine and mobile enough to be introduced in small quantities in available cavities between large particles according to the *insertion mechanism*. In the second case, the method consists in substituting some fine particles forming the matrix by a small quantity of spread large particles: this is the *substitution mechanism*. For a binary mixture "with geometrical interactions", the virtual packing density γ obtained by the CPM can be written as follows:

$$\gamma = \mathrm{Min}\left(\gamma_1 = \frac{\beta_1}{1-\left(1-\frac{\beta_1}{\beta_2}a_{12}\right)y_2} \; ; \gamma_2 = \frac{\beta_2}{1-\left(1-\beta_2+b_{21}\beta_2\left(1-\frac{1}{\beta_1}\right)\right)y_1} \right) \quad (1)$$

where γ_1 and γ_2 are respectively virtual packing densities of the binary mixture in the case "large grains dominant" and in the case "small grains dominant", β_1 and β_2 the virtual packing densities of the large size class 1 and of the small size class 2, y_1 and y_2 their volume fractions by reference of the total solid volume, a_{12} the loosening effect coefficient, b_{21} the wall effect coefficient. When the size ratio $x=d_2/d_1$ (fine/large) is equal to 1, a total interaction occurs:

$$b_{21}(1)=1 \text{ and } a_{12}(1)=1 \quad (2)$$

2.2 Real packing density of a binary mixture: compaction index.

The real packing density ϕ^* is calculated by introducing the compaction index K:

$$K = \frac{\frac{y_1}{\beta_1}}{\frac{1}{\phi^*}-\frac{1}{\gamma_1}} + \frac{\frac{y_2}{\beta_2}}{\frac{1}{\phi^*}-\frac{1}{\gamma_2}} \quad (3)$$

Because K is a representative value of the placing process, the expression (3) is an implicit equation of ϕ^*, with one and only one positive root. It can easily be solved numerically.

3 WALL EFFECT, LOOSENING EFFECT, INTERFERENCE EFFECT.

In figure 1 representative of "void ratio" ($e=1/\phi^*-1$) versus "volume fraction of small particles" for a binary mixture, the *insertion mechanism* is represented by the straight line AM and the *substitution mechanism* by the straight line FM. The wall effect is highlighted by FH section which is located above FO. Now, we are going to introduce the concept of interference effect wich is locally a loosening effect.

If we consider the "large grains dominant" area, the loosening effect is only localized around a particle insufficiently fine to insert into a cavity created by some touching larger particles. Interference effect is more global. If we consider the "small grains dominant" area, the effect of large particles is reduced to a wall effect if they are in small quantities troughout the matrix of fine elements. If their fraction increases, their relative position will have an influence: their walls will be too close to each other and they are going to interact on the arrangement of small particles. An interference will occur between the two components. Interference effect is materialized by the IKA section. It is locally called loosening effect in the AK section.

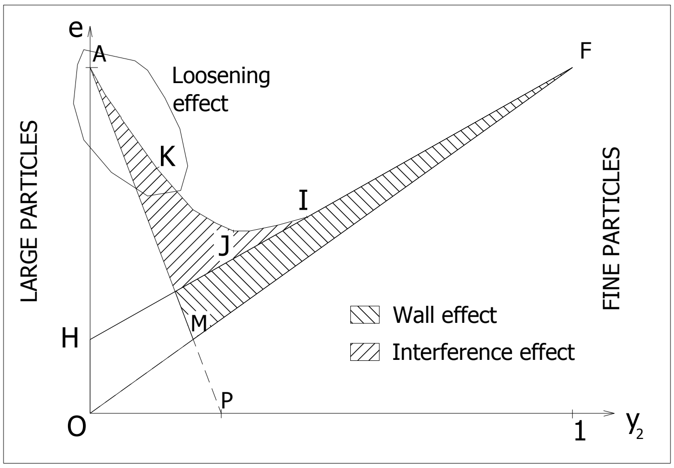

Figure 1. Illustration of wall effect, loosening effect, interference effect.

4 WALL EFFECT THEORY FOR SPHERES.

The wall effect has been the object of many experimental and theoretical studies: Ben Aim (1970), Stovall, de Larrard, Buil (1986), de Larrard (1988), de Larrard (2000). Ben Aim was a precursor in this domain. He considered that a planar wall effect is almost totally localized at the interface between the large and small spheres in a layer d/2 thickness (d: particle diameter). He generalises this way of reasoning to a curved wall. When he studies a large sphere of diameter d_1 surrounded by small ones of diameter d_2, he considers the wall effect disturbance in a portion delimited by two concentric spheres. The first one has a diameter d_1. The second hypothetical one is chosen in such a way that contact points between each small sphere pressed against the wall are located on its surface area. However, the boundary condition $b_{21}(1)=1$ is not respected. That's why we propose an adjustment of the Ben Aim reference cell:

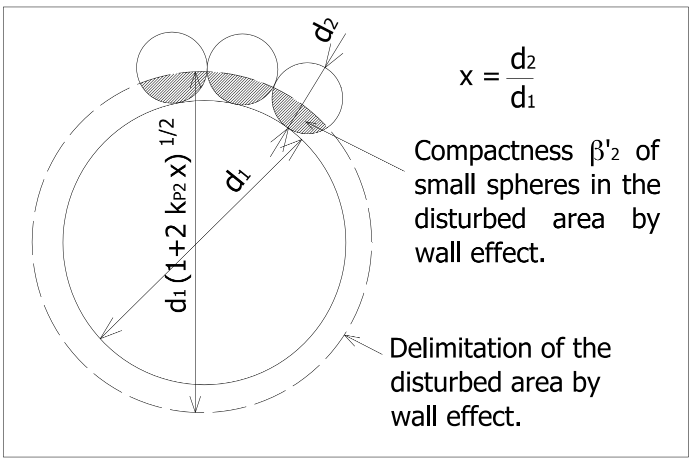

Figure 2. Definition of the spherical reference cell for studying the wall effect.

The diameter of the sphere delimiting the disturbed volume by the wall effect around a large sphere is:

$$d_{hyp} = d_1 \sqrt{1 + 2\,k_{P2}\,x} \tag{4}$$

Let α_2 be the real packing density of the fine class 2. We can deduce its virtual packing density β_2 by involving the compaction index K:

$$\beta_2 = \alpha_2 \frac{(1+K)}{K} \tag{5}$$

The number of small spheres against a large one is calculated from the spherical square model, not shown here, as part of the dense virtual packings:

$$N_{12,SSM}^{dense}(x) = \frac{\pi (1+x)}{x \arcsin\left(\frac{x}{1+x}\right)} \tag{6}$$

The packing density β'_2 of the small particles in the disturbed volume by the wall effect is deduced from this expression:

$$\beta'_2(x) = \frac{\pi(1+x)}{4\,x\left((1+2\,k_{P2}\,x)^{\frac{3}{2}} - 1\right)\arcsin\left(\frac{x}{1+x}\right)} \cdot \\ \cdot \left(2(1+2\,k_{P2}\,x)^{\frac{3}{2}} - 3(1+2\,k_{P2}\,x)\left(1+\frac{k_{P2}\,x}{1+x}\right) + \left(1+\frac{k_{P2}\,x}{1+x}\right)^3 - x^3 + \frac{3\,k_{P2}\,x^3}{1+x} + x^3\left(1-\frac{k_{P2}}{1+x}\right)^3\right) \tag{7}$$

In the case where $\beta_1=\beta_2$, the wall effect coefficient is expressed by:

$$b_{21}(x) = \frac{(\beta_2 - \beta'_2(x))}{(1-\beta_2)}\left[(1+2\,k_{P2}\,x)^{\frac{3}{2}} - 1\right] \tag{8}$$

It remains to be determined k_{P2} by respecting the boundary condition $b_{21}(1)=1$, leading to the numerical solution, by a spreadsheet program, or the analytical solution of the following equation:

$$(\beta_2 - 6)(1+2\,k_{P2})^{\frac{3}{2}} + \frac{9}{2}k_{P2}^2 + 18\,k_{P2} + 5 = 0 \tag{9}$$

The equation to be solved being of the 3rd degree, the value of k_{P2} which is coherent with those presented in the following table should be kept:

Table 1. Values of k_P as a function of the residual packing density β.

β	0,65	0,66	0,67	0,68	0,69	0,70	0,71	0,72	0,73	0,734
k_P	0,4466	0,5854	0,6729	0,7543	0,8369	0,9253	1,0252	1,1476	1,3284	1,4729

Here is a representative example of the wall effect coefficient b_{21} as a function of the size ratio x:

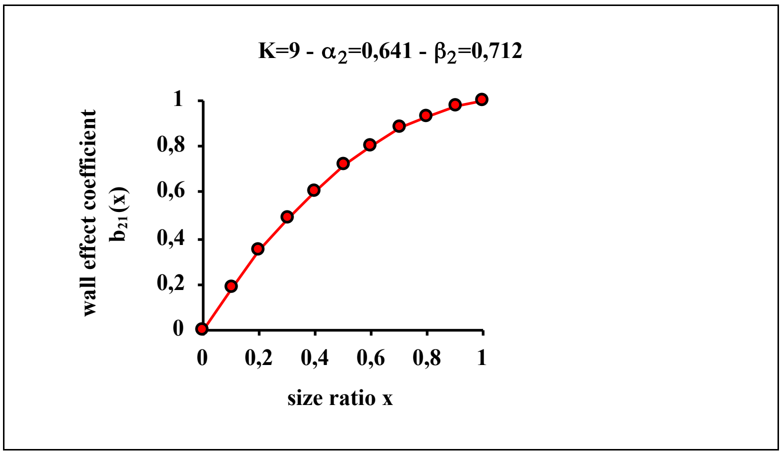

Figure 3. Representative example of the wall effect coefficient b_{21} for a real packing density of the fine class α_2=0,641, a compaction index K=9 and a residual packing density β_2=0,712.

5 LOOSENING EFFECT AND INTERFERENCE EFFECT THEORY FOR SPHERES.

Stovall, de Larrard, Buil (1986) introduced the concept of critical cavity size ratio x_0: below this value, the intrusion of small quantities of smaller spheres does not disturb the bed of larger spheres; beyond this value, small spheres cannot be placed without disturbing this one. Furthermore, when $x \rightarrow 1$, all particles become identical: calculated packing densities in the frame of the "small grains dominant" and in the frame of the "large grains dominant" must be equal when volume fractions of fine and large particles are 0,5. In addition to these two hypothesis, the concept of local isotropic expansion (de Larrard (1988)) of the large particle skeleton around a small one is adopted when $x>x_0$. But contrary to the original publication, a spherical reference cell is used for that, allowing to be consistent with the wall effect theory.

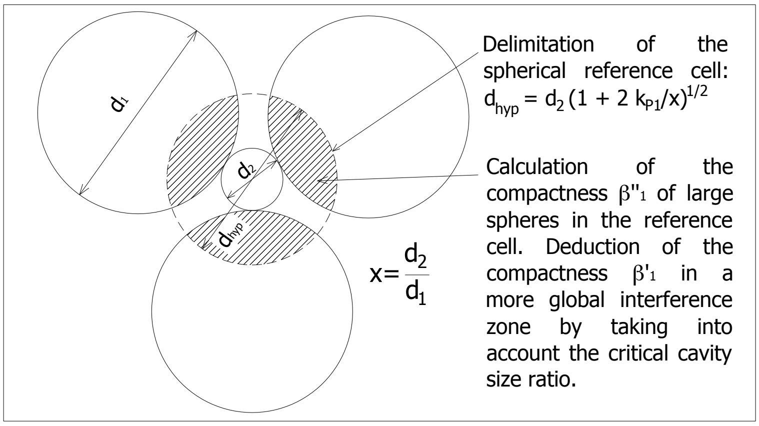

Figure 4. Definition of the spherical reference cell for studying the loosening effect.

The diameter of the sphere delimiting the disturbed volume by the loosening effect is:

$$d_{hyp} = d_2 \sqrt{1 + \frac{2\, k_{P1}}{x}} \tag{10}$$

Let α_1 be the real packing density of the large class 1. We can deduce its virtual packing density β_1:

$$\beta_1 = \alpha_1 \frac{(1+K)}{K} \tag{11}$$

The number of large spheres against a small one is calculated from the spherical square model:

$$N_{21,SSM}^{dense}(x) = \frac{\pi(1+x)}{\arcsin\left(\frac{1}{1+x}\right)} \quad (12)$$

The packing density β''_1 of the large spheres in the reference cell is:

$$\beta''_1(x) = \frac{\pi(1+x)}{4\left(1+\frac{2k_{P1}}{x}\right)^{\frac{3}{2}}\arcsin\left(\frac{1}{1+x}\right)} \cdot \left(2\left(1+\frac{2k_{P1}}{x}\right)^{\frac{3}{2}} - 3\left(1+\frac{2k_{P1}}{x}\right)\left(1+\frac{k_{P1}}{1+x}\right) + \left(1+\frac{k_{P1}}{1+x}\right)^3 - \frac{1}{x^3} + \frac{3k_{P1}}{x^2(1+x)} + \left(\frac{1}{x} - \frac{k_{P1}}{1+x}\right)^3\right) \quad (13)$$

The packing density of the large spheres in a more global interference zone is:

$$\beta'_1(x) = \frac{\beta''_1(x)}{\beta''_1(x_0)\left(1+\frac{(x-x_0)}{(1-x_0)}\left(\sqrt[3]{\frac{2\,\beta''_1(1)}{\beta''_1(x_0)}}-1\right)\right)^3}\,\beta_1 \quad (14)$$

When $x=x_0$, $\beta'_1(x_0)/\beta_1=1$: loosening effect and interference effect do not occur. When $x=1$, $\beta'_1(1)/\beta_1=0{,}5$: the continuity between "large grains dominant" and "small grains dominant" is provided when their volume fractions are equal and when all particles become identical. The volume fraction of small particles at the "eutectic" point, corresponding to the crossing point into the "small grains dominant" area, is:

$$\phi_2^*(x) = \beta_2 + \left((1-\beta_2)(1-b_{21}(x))-1\right)\beta'_1(x) \quad (15)$$

The loosening effect coefficient is deduced from this expression:

$$a_{12}(x) = \frac{\beta_1 - \beta'_1(x)}{\phi_2^*(x)} \text{ if } x \geq x_0 \text{ and } a_{12}(x) = 0 \text{ if } x \leq x_0 \quad (16)$$

k_{P1} remains to be determined by respecting the boundary condition $a_{12}(1)=1$ leading to solve the equation (9) by replacing k_{P2} by k_{P1} and β_2 by β_1.

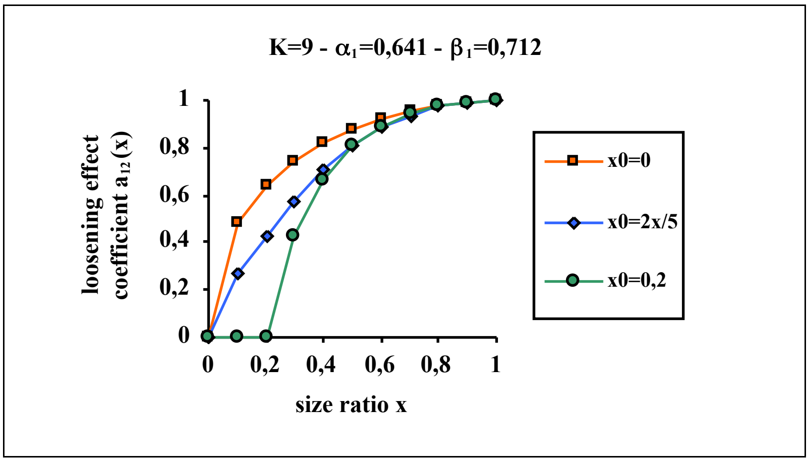

Figure 5. Representative example of the loosening effect coefficient a_{12} for $\alpha_1=0{,}641$, $K=9$, $\beta_1=0{,}712$ and critical cavity size ratios $x_0=0$, $x_0=0{,}2$ and $x_0=2x/5$.

6 THE 4-PARAMETER COMPRESSIBLE PACKING MODEL (CPM).

The compaction index K and the critical cavity size ratio x_0 need now to be calibrated by an analysis of 780 values on binary mixtures. x_0 is considered as a function of the type of aggregate, of its shape and of its finish surface.

Table 2. Compaction index K.

Packing processes	Pouring	Vibration	Vibration + compression	Optimized filling* + vibration + compression	virtual
K	**4,7**	**5,6**	**9**	**15**	**∞**

*The expression "optimized filling" corresponds to the use of a mixing chamber to fill the container by glass beads.

Table 3. Critical cavity size ratios x_0 (for natural aggregates, x: size ratio).

Type of aggregate	Crushed aggregate			Round natural aggregate	Frictionless glass beads
	Angular very rough	Angular rough	Angular		
x_0	**0**	**0,02**	**0,1**	**$x_0 = 2\ x / 5$**	**0,2****

**This value is very close to 0,2247 obtained for a tetrahedral cavern (Ben Aim (1970)).

Now, we are going to evaluate the 4-parameter CPM when compared to 780 results on binary mixtures. Data concerning glass beads come from the thesis of Ben Aim (1970) in which we can find results of Ben Aim; Mc Geary; Westman and Hugill; Tickell, Mechem and Mc Curdy; Naar, Wygal and Henderson; Yerazunis, Bartlett and Nissan and from experiments of Kwan, Chan, Wong (2013). Round natural aggregates are coming from the Loire (France) (de Larrard (2000)) and from the Seine (France): experimental results of Joisel given in the thesis of de Larrard (1988). Crushed aggregates are from the Pont-de-Colonne quarry at Arnay-le-Duc (France) (de Larrard (2000)), a soft limestone from Lorraine (France) (Lecomte and Zennir (1997)), a limestone aggregate from the northeast of Tlemcen (Algeria) (Hanini (2012)), a granite rock aggregate (Asia) (Kwan, Wong, Fung (2015)). Results of numerical simulation will be published in the thesis of Roquier at a later date.

The *4-parameter CPM* is evaluated by comparison of the *original CPM* and of the *original 3-parameter model* (Kwan, Chan, Wong (2013)) or *extended* (Kwan, Wong, Fung (2015)).

Table 4. Mean deviation ξ and correlation coefficient r on packing densities for various materials.

Models / Materials	**Original CPM**		**Original or extended 3-parameter model**		**4-parameter CPM**	
	ξ	**r**	**ξ**	**r**	**ξ**	**r**
Frictionless glass beads (300 values)	0,012	0,9754	0,009	0,9863	***0,007***	***0,9904***
Spherical particles numerically simulated (20 values)	0,012	0,8783	0,008	0,9598	***0,006***	***0,9877***
Round natural aggregates (125 values)	0,009	0,9619	0,012	0,9534	***0,007***	***0,9788***
Crushed aggregates (335 values)	0,013	0,9408	0,013	0,9455	***0,010***	***0,9642***

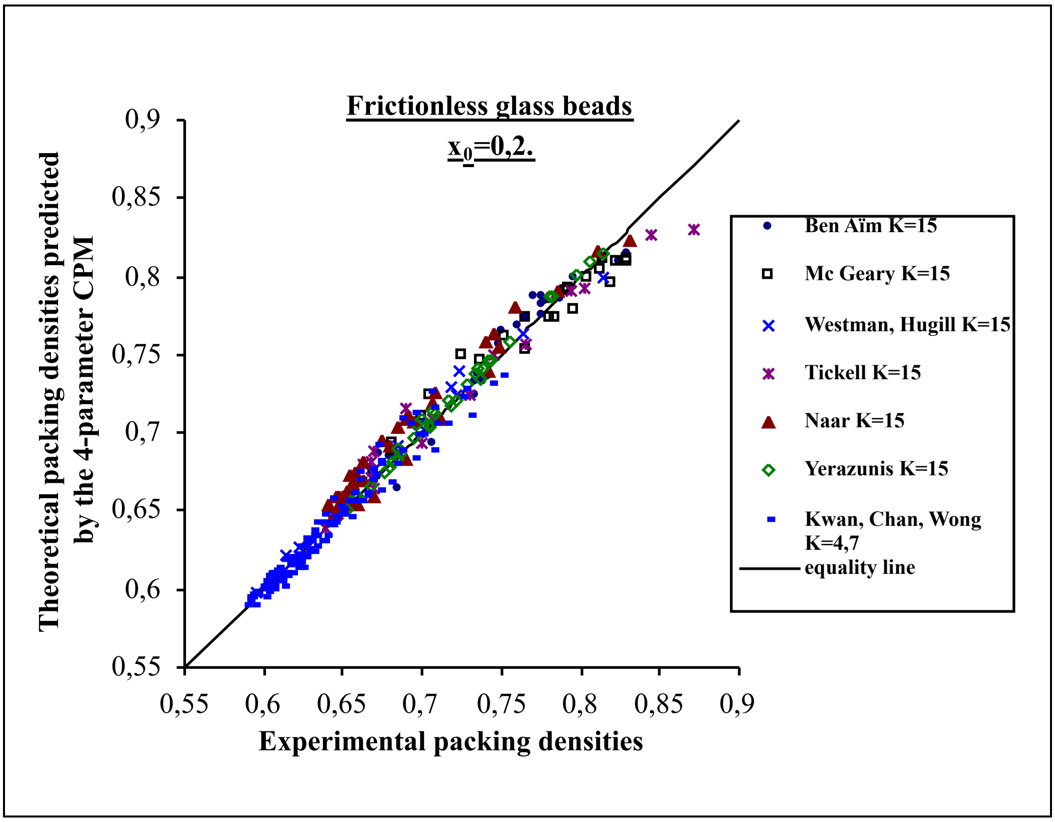

Figure 6. Experimental data compared with the 4-parameter CPM for frictionless glass beads.

7 VISCOSITY OF A BIDISPERSE SUSPENSION PREDICTED FROM THE 4-PARAMETER CPM.

A model intended to predict the viscosity of a bidisperse concentrated suspension with spherical, inert and rigid particles suspended in a Newtonian fluid is now presented. It takes into account geometrical and hydrodynamic interactions between particles. The fractal concept initially proposed by Farris (1968) is modified to include geometrical interactions used in the 4-parameter CPM. We have chosen a power-law relation (Krieger-Dougherty type) for the relative viscosity (Pabst (2004)). In the case $\beta_1=\beta_2=\beta$ (equal residual packing densities), the viscosity is calculated by:

$$\eta = \eta_0 \left(1 - \frac{\psi_1}{\psi_1^{MAX}}\right)^{-C_E\beta} \left(1 - \frac{\psi_2}{\psi_2^{MAX}}\right)^{-C_E\beta} \quad \text{with } d_1 > d_2 \tag{17}$$

$$\psi_1 = \phi\, y_1 \qquad \psi_2 = \frac{y_2}{\frac{1}{\phi} - y_1} \tag{18}$$

$$\psi_1^{MAX} = \frac{\beta\left(\frac{1}{\phi} - \frac{1}{\gamma_1}\right) + y_1\left(1-\beta\right)}{\frac{1}{\phi} - \frac{\beta}{\gamma_1}} \qquad \psi_2^{MAX} = \frac{\beta\left(\frac{1}{\phi} - \frac{1}{\gamma_2}\right) + y_2\left(1-\beta\right)}{\frac{1}{\phi} - \frac{\beta}{\gamma_2} - \left(1-\beta\right) y_1} \tag{19}$$

η is the suspension viscosity of the bidisperse suspension and η_0 the viscosity of the Newtonian suspending fluid.

ϕ is the volume fraction of the suspended spheres in a total volume unity, y_1 and y_2 the volume fraction of classes 1 and 2 by reference of the total solid volume, ψ_2 the volume fraction of the class 2 in a total volume unity, ψ_1 the volume fraction of the class 1 considering the presence of the finer class 2, ψ_2^{MAX} the maximal volume fraction of the class 2 in a total volume unity, ψ_1^{MAX} the maximal volume fraction of the class 1 considering the presence of the finer class 2, γ_1 and γ_2 respectively virtual packing densities of the binary mixture in the case "large grains dominant" and in the case "small grains dominant". C_E is equal to 2,5 in agreement with Einstein's relation for dilute suspensions.

This theory allows to highlight a new relation between relative viscosity and the volume fraction of the suspended spheres. When the latter reaches its critical value, the suspension is jammed and the mixture reaches the packing density of the solid skeleton.

8 CONCLUSIONS.

In twenty years, progress in basic and applied research has revolutionized concrete. The 4-parameter CPM is now able to analyze the concrete constituents packing at the level of particles which can be the micro level for the silica fume. It represents a useful tool in order to improve performance concrete such as mechanical strength by organizing the components so as to produce a denser material and to increase durability. One of these strongest qualities is that it is the result of a progression leading to a new theory on the wall effect and on the loosening effect. It includes the introduction of a critical cavity size ratio depending on the type of materials. This reveals that there would not be a single curve for geometrical interactions. Limitations of the proposed model are of two types. Firstly, the loosening effect appears, strictly speaking, from a threshold volume fraction. Secondly, the interaction coefficients are determined by considering the same virtual packing density for each granular class. However, the results obtained suggest that efforts will not have been in vain. By introducing science in concrete, concrete has become a high-tech material.

9 ACKNOWLEDGEMENTS.

Financial supports from the Association Universitaire de Génie Civil (AUGC, France) and from the chaire École des Ponts Paristech / Lafarge for the conference participation, are gratefully acknowledged.

10 REFERENCES.

Ben Aim R. (1970) *Étude de la texture des empilements de grains. Application à la détermination de la perméabilité des mélanges binaires en régime moléculaire, intermédiaire, laminaire*, Thesis attented at the Faculty of Sciences of the University of Nancy, France.

De Larrard F. (1988) "Formulation et propriétés des bétons à très hautes performances", *Rapport de recherche LPC*, n°149.

De Larrard F. (2000) "Structures granulaires et formulation des bétons", *Études et recherches des laboratoires des ponts et chaussées*, Ouvrages d'art OA34.

Farris R.J. (1968) "Prediction of the viscosity of Multimodal Suspensions from Unimodal Viscosity data", *Trans. Soc. Rheol.*, 12, (2), p.281-301.

Hanini W. (2012) *Étude de l'incidence de la granularité sur la compacité des mélanges granulaires*, Magister's dissertation in Civil Engineering. University Aboubekr Belkaid, Algeria.

Kwan A.K.H., Chan K.W., Wong V. (2013) "A 3-parameter particle packing model incorporating the wedging effect", *Powder Technology* 237, p.172-179.

Kwan A.K.H., Wong V., Fung W.W.S. (2015) "A 3-parameter packing density model for angular rock aggregate particles", *Powder Technology* 274, p.154-162.

Lecomte A., Zennir A. (1997) "Modèle de suspension solide et formulation de bétons calcaires en Lorraine", *Bulletin des laboratoires des ponts et chaussées* n°211, p.41-52.

Pabst W. (2004) "Fundamental considerations on suspension rheology", *Ceramics - Silikáty* 48 (1), p. 6-13.

Sedran T., De Larrard F., Angot D. (1994) "Prévision de la compacité des mélanges granulaires par le modèle de suspension solide", *Bulletin des laboratoires des ponts et chaussées*, n°194, p.59-86.

Stovall T., De Larrard F., Buil M. (1986) "Linear Packing Density Model of Grain Mixtures", *Powder Technology*, vol. 48, n° 1, p. 1-12.